

LITHIUM GADOLINIUM BORATE CRYSTAL SCINTILLATOR
FOR LOW FLUX NEUTRON DETECTION

by

Steven C. Howell

A senior thesis submitted to the faculty of

Brigham Young University

in partial fulfillment of the requirements for the degree of

Bachelor of Science

Department of Physics and Astronomy

Brigham Young University

April 2009

Copyright © 2009 Steven C. Howell

All Rights Reserved

BRIGHAM YOUNG UNIVERSITY

DEPARTMENT APPROVAL

of a senior thesis submitted by

Steven C. Howell

This thesis has been reviewed by the research advisor, research coordinator,
and department chair and has been found to be satisfactory.

Date

Lawrence Rees, Advisor

Date

Eric Hintz, Research Coordinator

Date

Ross Spencer, Chair

ABSTRACT

LITHIUM GADOLINIUM BORATE CRYSTAL SCINTILLATOR FOR LOW FLUX NEUTRON DETECTION

Steven C. Howell

Department of Physics and Astronomy

Bachelor of Science

Low flux neutron detection is challenging because of the low signal to background ratio. Lithium gadolinium borate crystal embedded in a plastic scintillator enhances low flux neutron detection through paired-pulse scintillation. The signal from this detector contains an energy pulse and a capture-gated pulse. To calibrate this new scintillator, a method was developed to recognize the neutron signal and extract the energy information. Progress was made toward finding the proper gains to calibrate the detector against an accepted standard.

ACKNOWLEDGMENTS

I would like to acknowledge and thank those who helped me through this process. I appreciate the mentoring of John Ellsworth, and Larry Rees serving as my advisor. I also appreciate Photogenics for inviting John and me to come to their facility and see how the scintillator was made as well as providing the documentation of the detector. Bart Czirr helped immensely in answering technical questions. I am grateful for the instruction and corrections provided by J. Ward Moody and Gus Hart. Most especially, I appreciate the BYU Physics and Astronomy department for the funding and support provided.

Contents

Table of Contents	vi
List of Figures	vii
1 Introduction	1
1.1 Challenges of neutron detection	1
1.2 Scintillation	2
1.2.1 Neutron scintillation	3
1.2.2 Li glass and liquid scintillator detector	4
1.2.3 ^6Li glass and plastic scintillator detector	5
1.3 LGB scintillator detector	5
1.3.1 Specifics of LGB scintillation	7
1.3.2 Calibrating the detector	8
2 Data Collection and Analysis	9
2.1 Initial hardware	9
2.2 Oscilloscope setup	10
2.2.1 Bunkers	11
2.3 Indoor practice field (IPF) measurements	12
2.3.1 Data acquisition	13
2.3.2 Separating the two pulses	14
2.3.3 Analyzing the IPF data	15
2.4 Compton edge of gamma ray signal	16
2.5 Early and late analysis	17
3 Results and Calibration	19
3.1 Preliminary results	19
3.1.1 Example	20
3.2 Future developments	21
Bibliography	23

List of Figures

1.1	Proton Recoil	3
1.2	LGB Scintillator	7
1.3	Californium Neutron Emission Spectrum	8
2.1	Characteristic Double-Pulse Neutron Signal	10
2.2	Indoor Practice Field	13
2.3	Histogram of IPF Data	15
2.4	Correlation for Equal Pulse Height of Electron and Proton Scintillations.	17
2.5	2d Plot of Pulses Using Areas.	18
3.1	Correlation for Equal Pulse Height of Gamma and Neutron Scintilla- tions with Extrapolation.	20
3.2	2d Plot of Pulses Using Areas with Regions Grouped.	21

Chapter 1

Introduction

1.1 Challenges of neutron detection

Nuclear physics had its beginnings in 1896 when radiation was first discovered. In 1932 neutrons were observed for the first time. Since that time, neutron detection has played a key role in shaping our understanding of nuclear physics.

Detecting neutrons is inherently difficult because of their neutral charge and the high background noise that can be encountered. Neutrons do not respond to electromagnetic fields eliminating all possibilities of directing their path or observing electromagnetic interactions. Neutrons are instead studied indirectly through secondary interactions with other particles. This brings inherent problems of noise. Beta particles, cosmic rays, and gamma rays mimic the interactions of neutrons. Shielding using lead or plastic eliminates alpha and beta particles, but gamma and cosmic rays penetrate the shielding. So even with shielding there is a need to differentiate neutrons from background noise.

1.2 Scintillation

Scintillation is a process used for detecting charged particle radiation. Scintillation occurs when an ionized atom emits a photon. Every scintillator emits at a characteristic wavelength determined by its chemical composition. This is also referred to as luminescence. Upon entering the scintillator, or luminescent material, particles transfer energy to the atoms of the material through collisions. This energy is then emitted through scintillations.

Scintillation occurs in a variety of materials with varying properties. An ideal scintillator exhibits the following qualities:

1. The material has a high efficiency of converting kinetic energy of charged particles into light.
2. The light output is linear with respect to the energy deposited for as large a range as possible.
3. The material is transparent to its own light emission spectrum.
4. The decay of the emitted light is fast enough to allow clear resolution between consecutive absorbed particles.
5. The material has good optical quality and is easily manufactured in practical sizes.
6. The index of refraction is close to that of glass (about 1.5) so it is easily coupled with other optical equipment.

In practice, no scintillator has all these qualities so materials are chosen which exhibit the most important ones for the specific application. [1]

1.2.1 Neutron scintillation

Neutrons do not interact directly with scintillators because they are not charged particles. To use scintillation for neutron detection, the scintillator material must be in an environment where neutrons transfer energy to charged particles. These are considered secondary reactions and can be detected using scintillation.

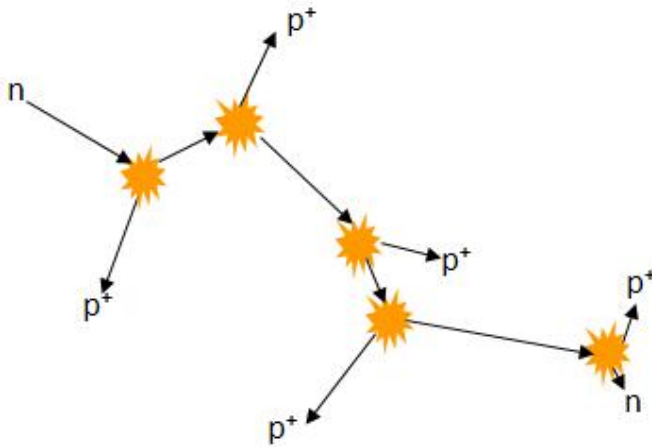


Figure 1.1 This depicts an energetic neutron losing its energy through proton collisions.

Organic scintillators accomplish this by having a high concentration of hydrogen. When a neutron collides with a hydrogen nucleus (or proton), energy is transferred. As depicted in Fig. ??, this happens several times until the neutron has lost most of its energy. The energetic protons interact with the scintillator emitting the energy as light.

The light is collected by a photomultiplier tube (PMT) as a single narrow pulse. A neutron's initial kinetic energy information is correlated to the intensity of that pulse. [2] To be effective, a PMT with a spectral sensitivity to the scintillator's characteristic wavelength is used.

Though these types of scintillators bypass the neutrality barrier, background radiation is still an issue. The gamma rays and cosmic rays, which cannot be efficiently shielded, also cause scintillation. The light output for gamma rays and neutrons is

similar making them hard to distinguish. [3]

Some inorganic scintillators overcome this background problem at the cost of interacting only with neutrons below a certain energy. One example is glass doped with lithium (${}^6\text{Li}$) deposits. When a neutron gets close enough to a ${}^6\text{Li}$ nucleus, if the momentum of the neutron is sufficiently low, the neutron can capture. Upon capture the neutron and ${}^6\text{Li}$ can undergo one of several reactions depending on the momentum. Two possible reactions are:



For the reaction in Eqn. 1.2, lithium has a capture cross section of $940b$ for $0.025eV$ neutrons. The more energy the neutron has, the higher it's momentum and smaller the ${}^6\text{Li}$ cross section, therefore the likelihood of this interaction happening decreases. This makes ${}^6\text{Li}$ a poor scintillator material for energetic neutrons.

1.2.2 Li glass and liquid scintillator detector

Since the 1980s, Bart Czirr and Gary Jensen from BYU as well as others have developed dual pulse scintillators through combining multiple scintillation materials. The first such detector was made from layering ${}^6\text{Li}$ glass and standard organic liquid scintillator. [4] [5] When an energetic neutron enters this detector, the cross section for ${}^6\text{Li}$ is extremely small because of the neutron's energy. The hydrogen-rich liquid absorbs the neutron energy, as described in section 1.2.1, causing an initial scintillation. Shortly after, a second scintillation occurs as the neutron is captured in ${}^6\text{Li}$. If an ambient low-energy neutron enters this detector, the cross section for ${}^6\text{Li}$ is large. But low-energy neutrons do not have enough energy to excite any hydrogen atoms; they capture on ${}^6\text{Li}$, only causing one scintillation.

This setup provides two unique signals for every energetic neutron that is detected. The first pulse is called the energy pulse because it provides energy information. The second pulse is the capture pulse and it provides a gate trigger. The capture pulse has a characteristic shape with a much longer decay time than the energy pulse. Gamma rays and cosmic rays cannot produce this capture pulse. Consequently every particle other than an energetic neutron only has one pulse. Through electronic analysis, the capture pulse paired with an energy pulse provides a discriminating gate. The processing program disregards single events or incorrectly pair dual events caused by gamma rays and from ambient low-energy neutrons. This is the first detector to provide information about a neutrons' energy and filter background radiation rather than measuring just neutron flux.

1.2.3 ^6Li glass and plastic scintillator detector

Wanting to improve upon the liquid glass detector, Bart Czirr and Eva Wilcox developed another detector using a standard plastic scintillator with ^6Li glass. They wanted to experiment with different numbers of glass layers, so the solid plastic made altering the setup a cleaner process. Other simplifications included using only one PMT and using a cylindrical casing. [6] [7]

1.3 LGB scintillator detector

Further development has led to a new scintillator which also exhibits the dual pulse of the liquid glass detector but with higher intensity light output. Bart Czirr and Photogenics found that cerium doped lithium gadolinium borate (LGB) crystals fluoresce much brighter than ^6Li glass. The LGB crystals are made from ^6Li , gadolinium (^{157}Gd), and boron (^{10}B) with an isotropic composition of $\text{Li}_6\text{Gd}(\text{BO}_3)_3:\text{Ce}$. [7] To

Sample	Amplifier Gain	Li Pulse Height	Li gain	B Pulse Height	B gain	Relative Brightness to Li Glass Cz/GS-20
GS-20 Li Glass	.40X300	259	2.158			
Cz272	.6X30	271	15.056	67	3.72	6.98
Cz274	.6X30	248	13.778	63	3.50	6.38
Cz275	.6X30	252	14.000	64	3.56	6.49
Cz283	.6X30	251	13.944	65	3.61	6.46
Cz277	.6X30	259	14.389	66	3.67	6.67
Cz278	.6X30	115	6.389	too low		2.96
Cz279	.6X30	249	13.833	63	3.5	6.41
Cz276A	.6X30	181	10.056	52	2.888889	4.66
Cz276B	.6X30	170	9.444	too low		4.38

Table 1.1 Relative brightness of lithium gadolinium borate crystal samples compared to ${}^6\text{Li}$ glass

quantify the relative brightness, crystals were tested at BYU Laboratory Nuclear Astrophysics Lab on 8 October 2007. The crystals were grown for Photogenics by the Institut de Chimie de la Matire Condense de Bordeaux, in France.

Lithium glass and thin slices of LGB crystals were each affixed with optical grease to the flat face of a PMT, placed in a dark box, and exposed to a californium (${}^{252}\text{Cf}$) source. The data in Table 1.1 were take with an ORTEC Trump MCA card and spectroscopy software. The LGB samples were 3 to 7 times brighter than ${}^6\text{Li}$ glass.

The scintillator for our detector is depicted in Fig. 1.2. All of the crystal samples tested except Cz278 and Cz276B were used to make the detector. The crystals were ground into micro-crystals then uniformly distributed in a common plastic scintillator, polyvinyl-toluene (PVT) doped with anthracene. The PVT plastic was made into a



Figure 1.2 This scintillator contains micro-crystals of lithium gadolinium borate cerium evenly dispersed in polyvinyl-toluene. (Picture compliments of Photogenics.)

cylinder 5 inches in diameter and 4 inches tall, containing 10% LGB by weight or 3% by volume. Attached to the scintillator was a photomultiplier tube (PMT) all inside a light tight aluminum container. [2]

1.3.1 Specifics of LGB scintillation

The signal for the LGB detector is similar to that of the liquid plastic scintillator with a few enhancements. Gadolinium plays a valuable role in enhancing the scintillation process producing the capture-pulse. Thousand of times per neutron, gamma rays from the second scintillation excite chains of ^{157}Gd transferring energy down the chain, similar to a bucket brigade. This chain is eventually broken when the energy interacts with cerium and emits as a visible photon. [2] This chain provides a slight delay between the two pulses and lengthens the capture pulse. The energy pulses we observe have a decay time between 20ns and 150ns, while the capture pulses have a decay time between 120ns and around $1\mu\text{s}$.

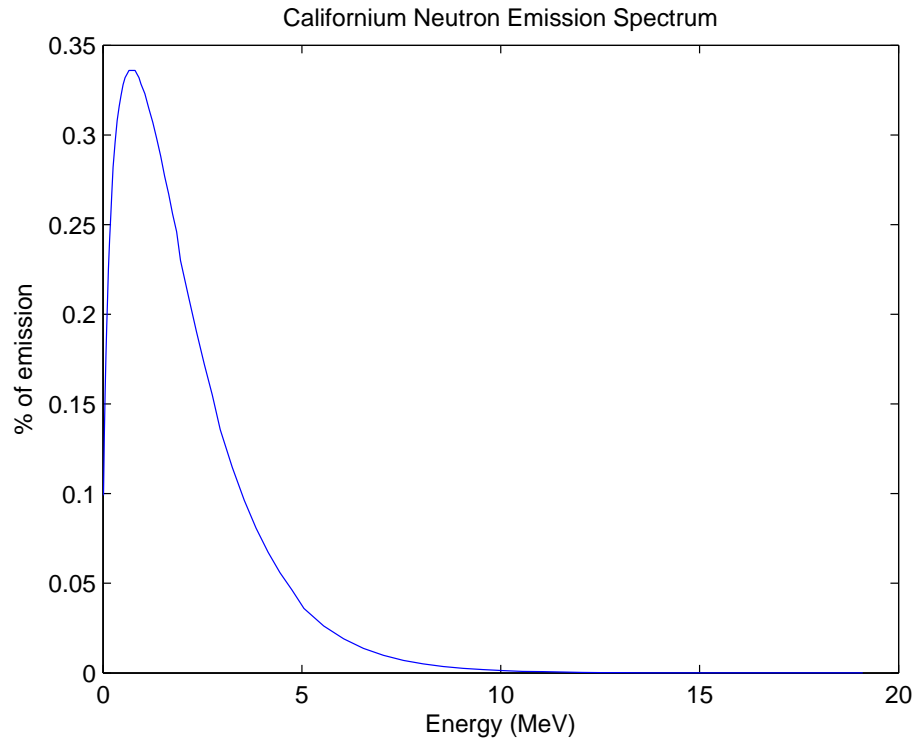


Figure 1.3 This is the spontaneous neutron emission spectrum of californium. [2] We are trying to reproduce this chart with the LGB spectrometer.

1.3.2 Calibrating the detector

The goal for this detector is to be used as a low flux neutron spectrometer. As mentioned, the height of the energy-pulse is correlated to the total energy transferred to the H atoms though it is not directly proportional to the energy. To convert pulse area into energy, we will study the signals obtained using universally accepted neutron and gamma sources.

Californium (^{252}Cf) spontaneously emits neutrons at energies depicted in Fig. 1.3. Our detector is sensitive to a similar range of neutron energies. Our goal is to reproduce this commonly known spectrum through actual measurements of a ^{252}Cf source.

Chapter 2

Data Collection and Analysis

Analyzing the signal from the detector is the first step toward calibration. After a scintillation, the PMT electronics convert the light into an analog voltage output. To analyze this signal with a computer, it must be converted into a digital signal. Once digitized, the characteristic dual pulse for a neutron can be found. Energy information is extracted by separating out the first pulse then integrating the signal to get the area of that pulse. From this point the proper gains may be applied to convert that area into neutron energy.

2.1 Initial hardware

We initially we used a LeCroy 6842 digitizer in a Camac crate to digitize the signal. The was signal transferred to the computer through a GPIB cable. A program for running this equipment was written in C code by David Buehler several years ago. Because of the dual signal we were looking for with the new LGB detector, the program had to be changed. Unfortunately, no one was familiar enough with the program and C code to make the needed changes.

To enable future students to more easily use the program, I attempted to translate the C code into a LabVIEW Virtual Instrument (VI). The VI was able to pass the desired settings to the digitizer, but it could never acquire data. Though the digitizer would arm, it could never store and pass a signal. The instrument documentation available was sparse and unhelpful, so after four months of little progress, we abandoned this project.

2.2 Oscilloscope setup

The next option for digitizing the signal was a Tektronix TDS3032C oscilloscope. I still had to solve the problem of triggering on the double pulse, though the oscilloscope provided more triggering options than the LeCroy digitizer. Using a threshold trigger, it was simple to pick out a energy-pulse or capture-pulse. Finding double pulses was more difficult. To record enough time before and after a single pulse, then to find the corresponding second pulse afterward would require so much sorting it would have

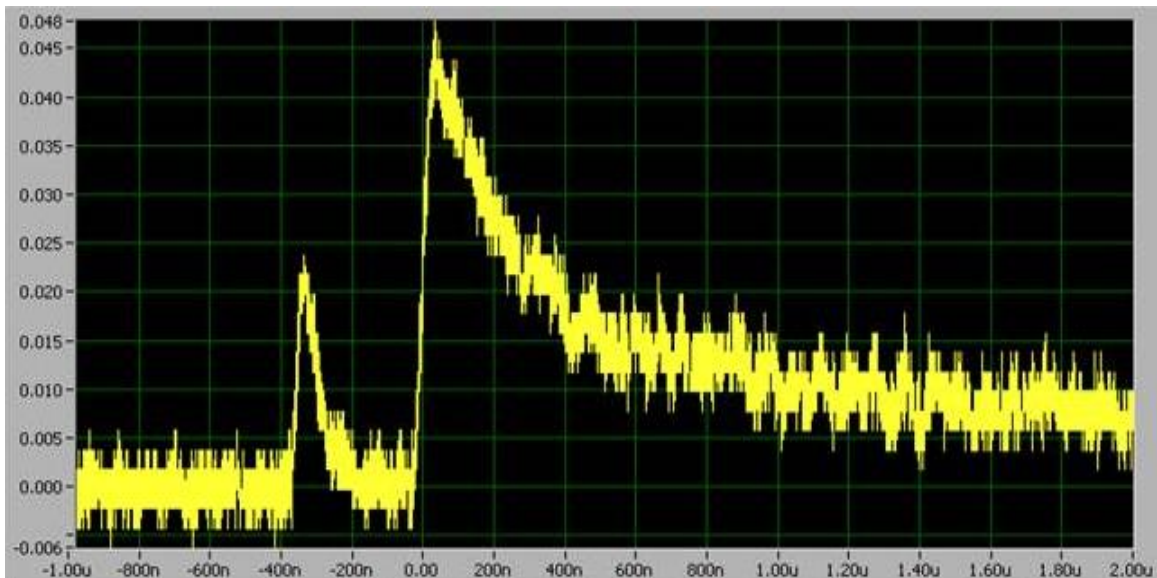


Figure 2.1 Characteristic double-pulse neutron signal. The valley between the two pulses enables dual-pulse triggering.

been unrealistic.

We wanted to find a way to trigger on the double pulse to minimize post processing. I found that I could do this using an inverted glitch trigger. This triggers on an inverted pulse within a certain width. Between two pulses, an inverted pulse is formed by the negative slope of the first pulse followed by the positive slope of the second pulse. We found that using $1.0\mu\text{s}$ as the maximum width between the pulses with a $3.0\mu\text{s}$ window gave good signals.

2.2.1 Bunkers

While we were setting up the triggering, we also experimented with different bunkers and their effects on the signals. To limit neutron exposure in the laboratory, bunkers were necessary to moderate or stop neutrons. About fourteen inches of moderating material is required to stop neutrons emitted from ^{252}Cf . Initially we used solid concrete blocks with a small horizontal well about two feet deep. Data were taken with the source placed deep in the opening with the detector upright about a foot from the opening.

A flaw in this setup was that with the neutrons directed at the side of the detector, the cross section for incoming neutrons was not uniform. A neutron directed straight through the center of the detector had 5 inches of scintillator to interact with. Changing the horizontal path angle just a little, significantly decreased the width the neutron passed through. At this stage, there was no need to change anything because we were only taking preliminary samples.

The second bunker was made from small blocks of paraffin (2 inches by 4 inches by 1/2 inch) packed closely in cardboard boxes. The boxes were arranged around the source and the detector with a clear path between the two. Our motivation for this bunker was to eliminate cosmic rays and ambient, low-energy neutrons. Cosmic rays

constantly shower down through our atmosphere with varied frequency. Low energy neutrons can be spontaneously emitted in small amounts from some materials.

Putting the source inside the bunker with the detector outside, we verified the paraffin was sufficiently thick to stop neutrons. On the other hand, looking at the single pulses from gamma rays, there was no visible difference in the count rate using the paraffin.

Though the paraffin did stop ambient neutrons, it did not shield gamma rays and it enhanced error from room return. Room return is when a detected neutron had collided with a wall or some moderating material (like paraffin) losing energy before being detected. When accurate energy measurements are important, this must be minimized. The paraffin enhanced room return increasing the probability that neutrons would reflect into the detector.

2.3 Indoor practice field (IPF) measurements

Because the bunkers did little to decrease background, we focused on decreasing room return. To eliminate room return, the source and the detector should be far from any solid material.

Depicted in Fig. 2.3, the Brigham Young University Indoor Practice Field (IPF) is over 100 yards by 50 yards of indoor field with a roof at least 100 feet high. By suspending the detector from the rafters and the source from the detector, we were able to take measurements with less than 1% probability of reflected neutrons reaching the detector. [2]



Figure 2.2 On the left is a wide view of the setup inside the indoor practice field. This shows how large the building is. On the right is a close-up of the detector and source configuration. We oriented the detector so the incident neutrons were directed at the flat side.

2.3.1 Data acquisition

On 19 January 2009, we recorded 5000 events using a ^{254}Cf source in the IPF. The VI for storing the data was created by modifying a sample VI provided on the National Instruments' web page.

Before modification, the sample VI would simply read in the current signal from the oscilloscope. I altered the program to repeat this process for an adjustable number of iterations. The VI would read in the current signal as fast as it could store it in the computer's memory. After completing the iterations, the VI would then store this data to the hard drive. Because the VI was not linked to the scope's trigger, we frequently digitized the same signal more than once. It was also possible to miss

signals while the computer was processing. We plan to address this issue in the future, but at this stage we ignored identical consecutive signals. After taking out repeated pulses we were left with 1959 unique double-pulse pairs.

2.3.2 Separating the two pulses

After capturing neutron signals, our next goal was to identify the energy. The analysis of the energy-pulse was challenging because the timing of the pulses vary. The energy pulse was not always at the same time in the $3.0\mu\text{s}$ window which meant the time between pulses changed. Additionally, the decay time varied depending on the intensity of the pulse. I needed to find a way to separate out each of the two pulses to enable analysis.

In order to accomplish this, I developed a VI using min and max values that isolated the two signals and then determined if they represented the characteristic signal. The only input required for the VI was to specify where in the 10,000 points the scope had triggered. From that point, the VI split the signal at the minimum between the two pulses. The VI would then find the max value before and after that dividing point. From each of these maximums, the VI identified where the pulse crossed 0.3 of the max. This defined the beginning and end of each pulse. The VI would store in Excel the width (in time) for each pulse at 0.3 of the max, the area of the first pulse, and whether the signal met the qualifications of a characteristic signal. A good signal met all the following criteria:

1. Time between the two pulses was greater than 4ns.
2. Time between pulses was less than 800ns.
3. The duration of the 1st pulse was less than 120ns.
4. The duration of the 2nd pulse was greater than 120ns.
5. After the 2nd pulse the signal remained below $2/3$ of the 2nd peak's max.

6. Before the 1st pulse the signal remained below $1/2$ the 1st peak's max.

The first and second criteria ensured the signal was a real dual pulse and the signals were close enough to attribute to an actual neutron. The third and fourth criteria ensured the first signal was an energy pulse and the second was a capture pulse. The fifth and sixth criteria ensured there were only two pulses and not three or four pulses in the same signal. After applying these conditions, 1484 of the 1959 unique signals qualified as neutrons.

2.3.3 Analyzing the IPF data

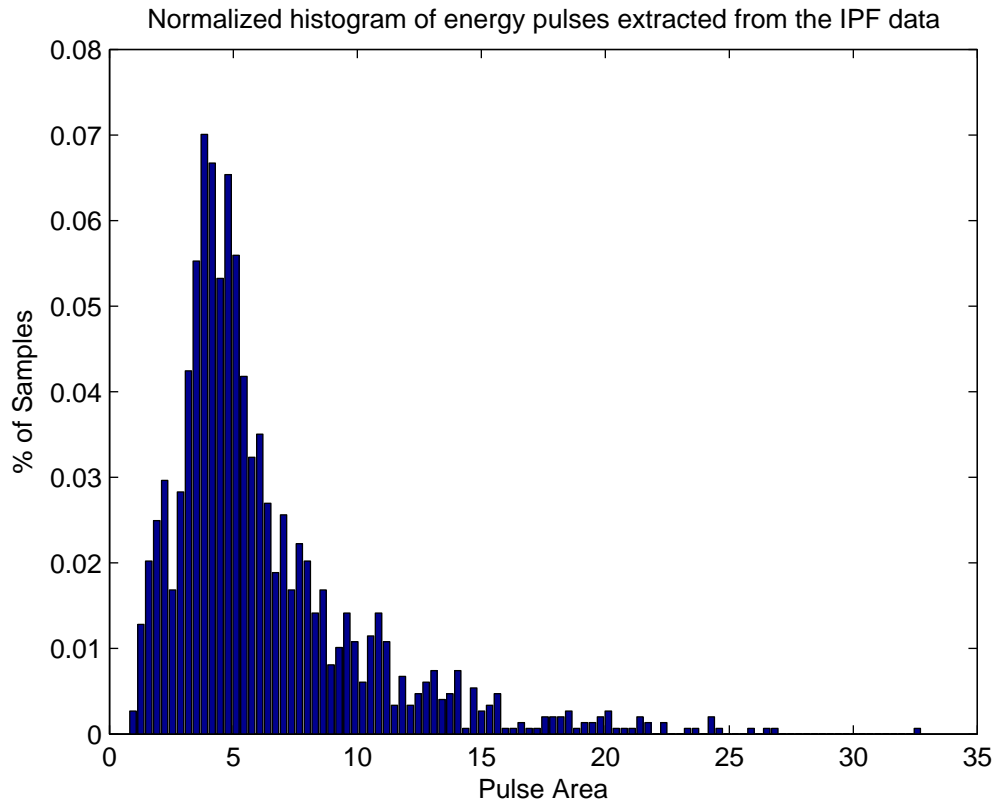


Figure 2.3 This is a histogram of the 1484 energy-pulses extracted from the IPF data. The area of pulse is correlated to neutron energy.

There was a definite correlation between the IPF data in Fig. 2.3 and the spectrum of the source in Fig. 1.3. Different calibration factors lead to a closer match between the spectrum and the histogram.

Simply using multiplicative factors to improve this match ignored detector efficiency. The more energy a neutron has, the higher the probability that it will pass through the detector before losing enough energy to be captured. A crude relation for this probability of being captured is the inverse of the energy. [2] We were unsure how to apply this, though, and began looking for other means of calibration.

2.4 Compton edge of gamma ray signal

After little success matching the data from a wide spectrum source, we wanted to use distinct energy sources instead. We had two such gamma sources, cobalt (^{60}Co) and cesium (^{137}Cs). Cobalt emits gamma rays at energies of 1.1732 MeV and 1.332 MeV. Cesium emits gamma rays at energies of 0.6616 MeV, 31.8 keV and 32.2 keV. [1] From Bart Czirr, we learned the correlation between pulse height of gamma signals and neutron signals shown in Fig. 2.4. From analyzing the Compton edge for the two source we anticipated finding two reference points to correlate neutron and gamma scintillations. Using the data shown in Fig. 2.4 we would know the energy for two different neutron scintillations. [2]

I took 4000 unique samples with ^{60}Co and another 8000 samples with ^{137}Cs . To compare these spectra with the background, I took another 4000 samples with no source. We wanted to ensure that the high incidence rate of background gamma rays did not mask the data. Their histograms showed similarities but exhibited clear differences as well. Unfortunately, relying on the Compton edge from the plastic scintillations proved non-conclusive. The detector could not resolve the gamma rays

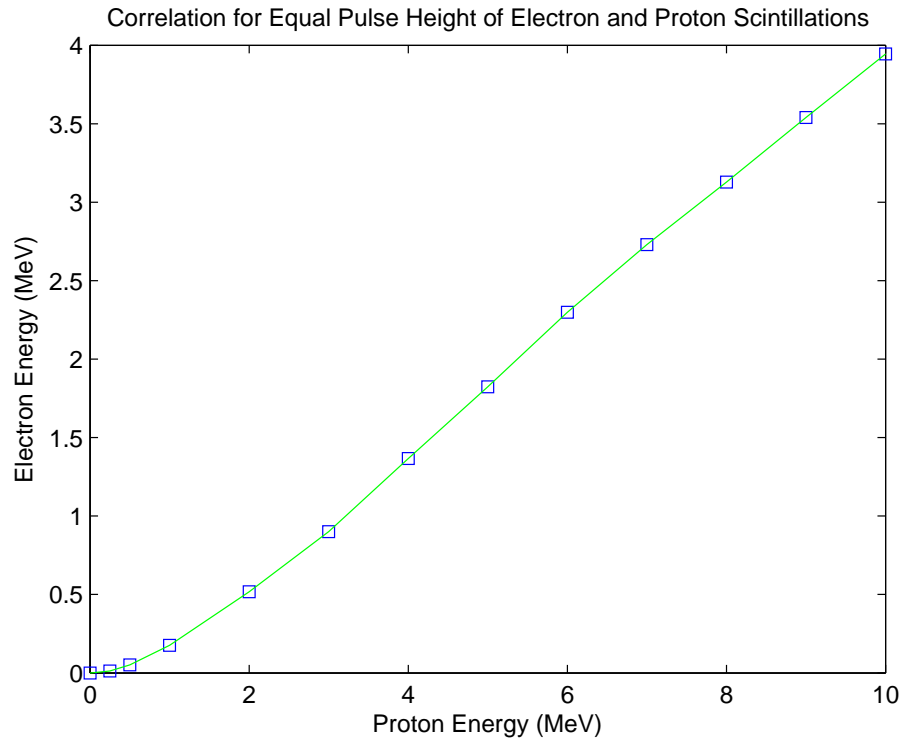


Figure 2.4 This curve shows the correlation between a proton and an electron scintillation. Along the curve the two reactions will have the same light output. The squares depict actual measured correlation points between the two. [2]

accurately so we abandoned this effort.

2.5 Early and late analysis

Figure 2.5 depicts a two-dimensional plot of the separated pulses. To do this I defined an early and late time window as 300ns and 700ns, respectively. I then took the area of every pulse within those two windows. I plot the early area divided by the total area against the total area. By the end of the early window, energy pulses have decayed close to zero. Consequently, the ratio of the early area to total area is nearly one. The capture pulses, on the other hand, have significant area in both the early

and late window.

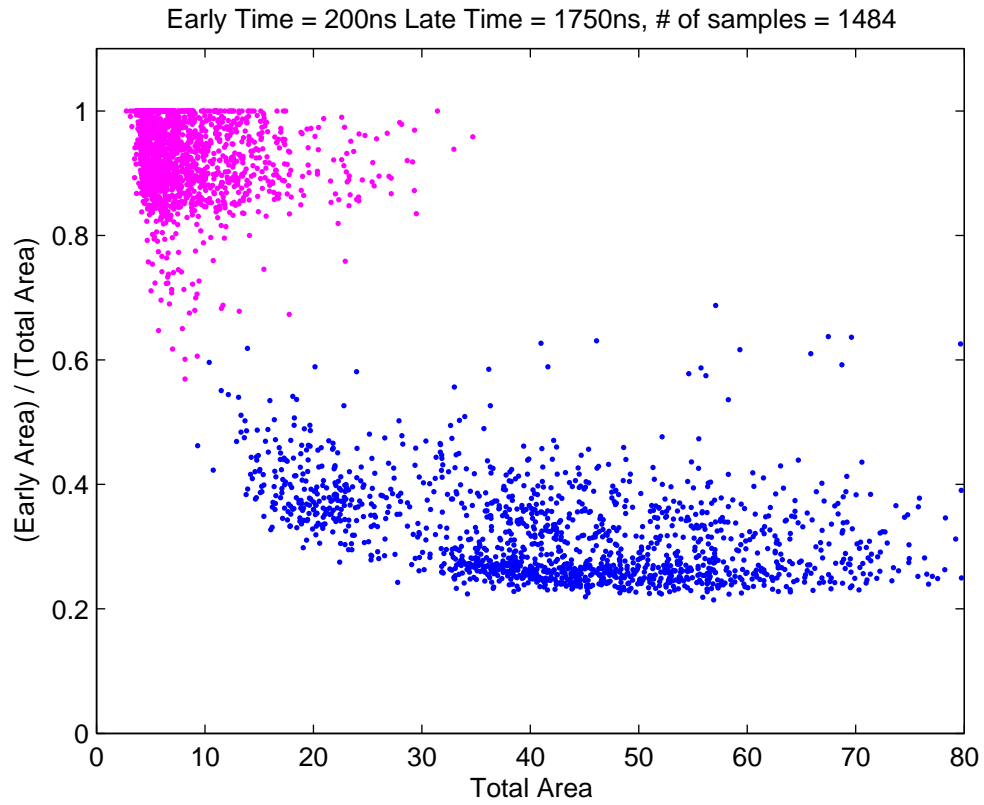


Figure 2.5 2d plot of pulses using early and late areas.

Chapter 3

Results and Calibration

3.1 Preliminary results

Since the energy of gamma rays emitted from neutron capture is known, comparing the capture and energy pulses can give us the correlation necessary to calibrate the detector. Inspection of the Fig. 2.5 shows grouping of data in certain areas. We expected this when considering the different energy released depending on if the neutron captured on ${}^6\text{Li}$, ${}^{157}\text{Gd}$, and ${}^{10}\text{B}$.

With a Monte Carlo simulation and a chart like Fig. 2.5, we would know where to expect capture pulses on ${}^6\text{Li}$, ${}^{157}\text{Gd}$, and ${}^{10}\text{B}$. The simulation would also tell us what the relative strengths should be. The area for the center of these regions would correspond to the gamma emitted from each capture. We could then correlate the total peak area with the gamma ray energy. This means that the gamma energy as a function of the total peak area becomes self calibrating.

If the neutron's energy pulse could be attributed to only a single excited proton, we could deduce the proton's energy from Fig. 2.4. This would also be the neutron's energy prior to colliding with the proton. The process is actually more complicated

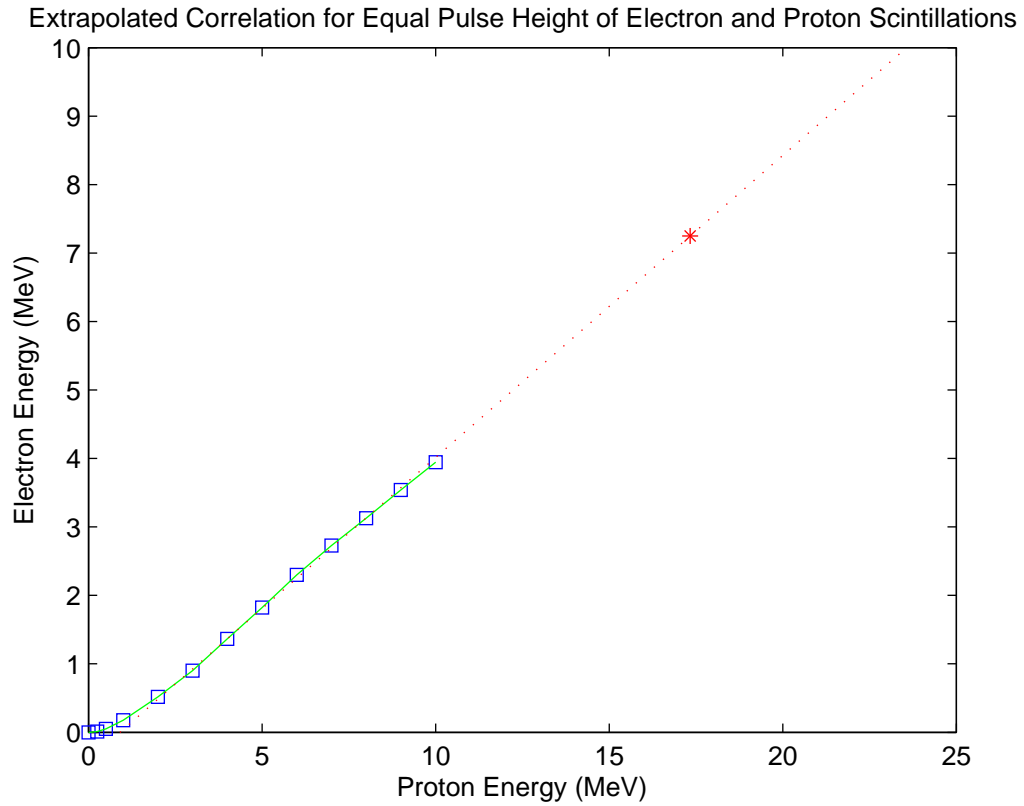


Figure 3.1 This show an extrapolation of Fig. 2.4 to 7.25MeV gamma ray energy.

because the neutron collides with multiple protons and the curve in Fig. 2.4 is non-linear. We then input Fig. 2.5 and the known ^{254}Cf spectrum into the Monte Carlo simulation to obtain the predicted response. This would hopefully match the measured data from our IPF measurements.

3.1.1 Example

An example of how this would work is as follows. Lets assume the region 3 of Fig. 3.2 represents neutron captures on the ^6Li . The center of this is at an area of approximately 45. If we also assume the capture follows the branch diagramed in Eqn. 1.1, we would know the area of a 7.25MeV gamma is 45. By extrapolating the data from

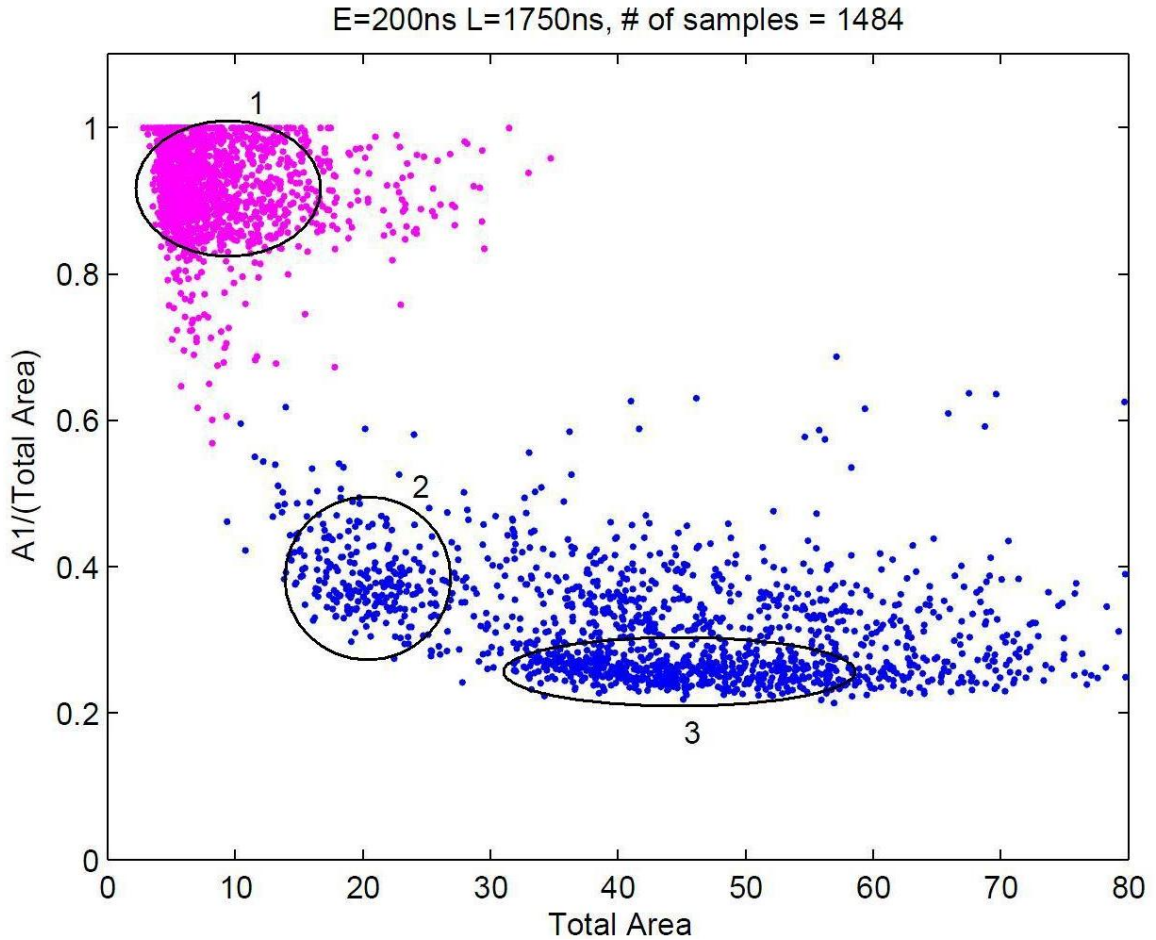


Figure 3.2 2d plot of pulse areas with regions grouped. In region 1, the early area over the total area is approximately 1. This is what we expect for energy pulses. It is likely region 2 represents boron capture

Fig. 2.4 up to 7.25MeV electron energy we get Fig. 3.1. From this figure we deduce that a single proton with about 17.3MeV would be required to create a pulse of the same area as the 7.25MeV gamma.

3.2 Future developments

Effective use of this detector depends on the ability to reduce the dead time caused by the time required for the VI to process each signal. As mentioned, using the

oscilloscope rather than the digitizer slowed the response time. As currently setup, dead time is beyond what would be reasonable for practical applications. To speed up the detection process, there are plans to design a circuit which will incorporate the energy calibration into an on the fly processing system. The circuit programming will be setup to recognize the form of the capture pulse. Simultaneously, the signals will be pre-processed into modified gaussian pulses whose peak corresponds to the energy. When a capture-pulse is found, the circuit will look at the preceding pulse to find the energy. The only output will be a number representing the energy of the excited protons. In post-processing, the neutron distribution related to that proton energy can be applied.

Bibliography

- [1] G. F. Knoll, *Radiation Detection and Measurement*, 3rd ed. (Wiley, New York, 1999), pp. 219,445.
- [2] J.Bart Czirr (private communication).
- [3] J Ellsworth (private communication).
- [4] G. L. Jensen, D. R. Dixon, K. Bruening, and J. B. Czirr, “A moderating ^6Li -glass neutron detector,” *Nuclear Instruments and Methods in Physics Research* **220**, 406 – 408 (1984).
- [5] J. Czirr and G. L. Jensen, “A neutron coincidence spectrometer,” *Nuclear Instruments and Methods in Physics Research Section A: Accelerators, Spectrometers, Detectors and Associated Equipment* **284**, 365 – 369 (1989).
- [6] E. Wilcox, “Novel neutron detector for n-n scattering length measurement,” Masters Thesis (Brigham Young University, Provo, U.T., 2005).
- [7] J. B. Czirr, D. B. Merrill, D. Buehler, T. K. McKnight, J. L. Carroll, T. Abbott, and E. Wilcox, “Capture-gated neutron spectrometry,” *Nuclear Instruments and Methods in Physics Research Section A: Accelerators, Spectrometers, Detectors and Associated Equipment* **476**, 309 – 312 (2002).